The A-State of Barnase†

Jesús M. Sanz,‡ Christopher M. Johnson, and Alan R. Fersht*

MRC Unit for Protein Function and Design, Cambridge Centre for Protein Engineering, Medical Research Council Centre, Cambridge CB2 2QH, U.K.

Received May 18, 1994; Revised Manuscript Received July 19, 1994®

ABSTRACT: The acid-induced denaturation of barnase and its mutants has been analyzed to search for partly-folded intermediates. Differential scanning calorimetry of barnase deviates from two-state behavior below pH 4.0 at low ionic strength, with the maximum discrepancy at pH 2.7. Addition of 200 mM KCl apparently restores the two-state transitions. Thermograms of barnase mutants at pH 2.7 and low ionic strength fall into three classes: *a*, symmetric transitions which fit well to a two-state equilibrium; *b*, asymmetric transitions indicating deviation from two-state behavior; and *c*, transitions with an obvious second component. The most distorted thermograms are observed for mutants that had previously been engineered to accumulate at equilibrium the major kinetic folding intermediate state of barnase at neutral pH. Further analysis of these mutants show the existence of complex equilibria on thermal denaturation. Addition of KCl leads to the slow formation of soluble aggregated forms (A-state) which share some of the properties of the "molten globule" state, *i.e.*, significant secondary structure, lack of fixed tertiary structure, and solvent-accessible hydrophobic patches. The far-UV CD spectrum of the A-state can be explained in terms of native-like secondary structure contributions. Kinetic and chemical cross-linking experiments show that dimerization of partly-folded molecules occurs in the transition region, and such dimerization is probably the rate-limiting step in the formation of the A-state in the presence of KCl. As the A-state has been oberved clearly so far for only the mutants in which the folding intermediate has been designed to accumulate, we suggest that the A-state would be related to the main folding intermediate state of barnase. The intermediate would be highly stabilized at low pH, and it is prone to self-associate in these conditions.

Characterization of intermediates during protein folding is an essential step in understanding folding pathways. Such intermediate states are increasingly the subject of study (Dill, 1985; Ptitsyn, 1987; Oas & Kim, 1988; Kuwajima, 1989; Kim & Baldwin, 1990) although a detailed analysis remains mainly elusive. The intermediates are usually metastable and short-lived under conditions normally used to monitor folding (*i.e.*, pH close to 7 and physiological ionic strength and temperatures). Accumulation of these species at equilibrium has already been achieved by covalent trapping (Creighton, 1986) and protein engineering (Hughson et al., 1991; Sanz & Fersht, 1993), but most studies are performed at extremes of pH, with mild denaturant concentrations, or in the presence of solvents that stabilize the intermediates, leading sometimes to the appearance of the so-called "molten globules", "collapsed forms", or "compact intermediates" (Ptitsyn, 1987; Kuwajima, 1989; Creighton, 1990; Goto et al., 1990; Bychkova & Ptitsyn, 1993). These forms have been termed "A-states" when obtained at low pH (Kuwajima, 1989). They usually show little, if any, cooperativity upon thermal denaturation (Yutani et al., 1992; Griko et al., 1994; Griko & Privalov, 1994) although it has been shown that a significant cooperativity is possible in theory (Haynie & Freire, 1993) and has been observed in practice (Bychkova et al., 1992; Kuroda et al., 1992). Whether or not these A-states are true folding intermediates is of interest. However, this link has only had indirect confirmation in some cases (Kuwajima et al., 1985; Sugawara et al., 1991; Barrick & Baldwin, 1993; Jennings & Wright, 1993), whereas in others it has been found that these species do not seem to be on the folding pathway but rather are alternatively folded structures (Buchner et al., 1991; Khurana & Udgaonkar, 1994).

The folding pathway of the ribonuclease from *Bacillus amyloliquefaciens* (barnase) involves a kinetically significant intermediate that accumulates transiently (Matouschek et al., 1990, 1992a). The structure of this intermediate has been mapped in considerable detail from a kinetic analysis of a large number of mutants (Matouschek et al., 1992a) and has been engineered to accumulate at equilibrium in the presence of certain concentrations of urea (Sanz & Fersht, 1993). From both studies it can be concluded that the intermediate has a significant degree of secondary structure, a partially formed hydrophobic core, and an incomplete tertiary structure.

In this article we study the thermal unfolding of barnase at low pH in order to examine possible A-states of this protein. In an effort to establish a correlation between the conformational states found under these conditions and the kinetic folding intermediate, we have included the study of several mutants of barnase which are known to accumulate the folding intermediate at equilibrium to some extent (Sanz & Fersht, 1993). As a preliminary definition, we would like to distinguish between the terms "denatured" and "unfolded". We use "denatured" to designate those states that are non-native, irrespective of the degree of unfolding. Any partly folded intermediates will be included in this terminology.

MATERIALS AND METHODS

Materials. The buffer used in these studies, unless otherwise stated, was 20 mM glycine hydrochloride, pH 2.7 (glycine buffer or low ionic strength buffer, hereafter). This was prepared by dilution from a stock solution containing 1 M glycine (Sigma) and 0.42 M HCl. SP-Trisacryl was obtained from IBF, Villeneuve la Garenne, France. *Escherichia coli*

†J.M.S. is supported by EMBO.

* To whom correspondence should be addressed.

‡ Present address: Departamento de Estructura y Funcion de Proteinas, Centro de Investigaciones Biologicas (CSIC), Velázquez 144, 28006 Madrid, Spain.

® Abstract published in *Advance ACS Abstracts,* September 1, 1994.

0006-2960/94/0433-11189$04.50/0

BL21(DE3) (pLysS) was a generous gift from Dr. F. W. Studier. 1-Anilinonaphthalene-8-sulfonic acid (ANS)[1] was from Molecular Probes, Inc. Covalent cross-linking of barnase was performed with the bifunctional agents formaldehyde (BDH), glutaraldehyde, and 1-ethyl-3-[3-(dimethylamino)-propyl]carbodiimide (EDAC) (Sigma).

Expression and Purification of Barnase. Wild-type barnase and its mutants were expressed in *E. coli* BL21(DE3) (pLysS) cells harboring a pTZ18U plasmid containing the barnase gene and purified as previously described (Serrano et al., 1990; Sanz & Fersht, 1993).

Differential Scanning Calorimetry. Samples for calorimetric analysis were generally dialyzed extensively against the appropriate buffer at 4 °C and then centifuged at 13 000 rpm in an MSE microcentrifuge for 10 min. However, identical results were obtained when samples were prepared without dialysis from concentrated stock solutions of protein in H_2O and buffer. Protein concentrations were determined from absorbance measurements assuming an extinction coefficeint of 27 364 M^{-1} cm^{-1} at 280 nm. This value has been determined for a number of barnase mutants and is within error of the wild-type value except for mutations involving Trp and Tyr (Vuilleumier et al., 1993). Consequently, an extinction coefficient of 24 628 M^{-1} $cm^{-1}$was used for all proteins with the Y78F mutation. DSC measurements were performed using a Microcal MC-2D instrument using the notional scan rates indicated in the text. The instrument uses a constant power system, and the true scan rates were always within 10% of the indicated values. All samples were degassed under vacumn with gentle stirring for 2–3 min before loading and were held under 2 atm of N_2 pressure during scanning. Samples that were rescanned were cooled *in situ* over a period of 50 min before a repeat scan was performed.

DSC thermograms were corrected by subtraction of the appropriate buffer base line and converted to excess heat capacity using the measured protein concentration and the cell volume supplied by the manafacturer. The heat capacity increment on denaturation was eliminated using an interpolative base line between the pre- and post-transitional heat capacity slopes in proportion to the progress through the transition. No other processing or smothing of the data was performed. Analysis of the resultant thermograms to two-state and non-two-state transitions was performed using Microcal Origin software (v. 1.16, Microcal Software Inc.) which is based on standard deconvolution procedures.

Thermal Denaturation Followed by Fluorescence Spectroscopy. Changes in the intrinsic fluorescence of barnase upon thermal denaturation were followed in an Aminco Bowman Series 2 spectrofluorimeter (American Instruments Co.) with excitation at 290 nm (bandpass = 2 nm) and emission at 315 nm (bandpass = 8 nm). The temperature was measured with a thermocouple immersed in the cuvette above the light beam. Rescans of the samples were completely reversible, ruling out photolysis events. To monitor the binding of ANS, up to 2 μM barnase was incubated at 5 °C with 40 μM of the ligand for 30 min prior to increasing the temperature. ANS fluorescence was measured on excitation at 380 nm and emission at 480 nm. The possibility of precipitation was checked by centrifuging the samples after addition of ANS (MSE microcentrifuge 13 000 rpm for 5 min) and comparing the fluorescence of the protein and ANS before and after the centrifugation.

Circular Dichroism. CD measurements were made in a Jasco J-720 spectropolarimeter fitted with a thermostated cell holder and interfaced with a Neslab RTE-110 water bath. Spectra were acquired at a scan speed of 50 nm/min and averaging at least 6 scans. The response time was 2 s. Ellipticities are expressed in units of deg cm^2 $dmol^{-1}$ using the mean residue concentration in the far-UV or the protein concentration in the near-UV experiments. When the scans were taken of oligomeric associates, we quote the initial monomer concentration. For all CD spectra a buffer base line was subtracted. Thermal denaturation experiments were performed at heating rates of 50, 20, and 10 °C/h, using a response time of 2, 4, and 8 s, respectively. Secondary structure contributions to the far-UV CD spectrum of barnase were calculated according to the parameters of Bolotina et al. (1980).

Size-Exclusion Chromatography. Gel filtration chromatography was performed using either a Superdex G-75 FPLC gel filtration column (10 × 300 mm) (Pharmacia) or a Tosoh G-2000 PW HPLC gel filtration column (Gilson), equilibrated in glycine buffer plus 200 mM KCl. Samples of barnase were prepared in the same buffer as present in the column, centrifuged (MSE microcentrifuge, 13 000 rpm, 5 min), and then applied to the column.

Kinetic Analysis of the Formation of the A-State. The time course of the formation of the A-state of barnase was followed by monitoring the changes in ellipticity at 222 nm. The protein in glycine buffer was equilibrated at the desired temperature. Then 200 mM KCl was added, and the reaction mixture was added to the CD cuvette which was also equilibrated at the same temperature. Manual manipulations took about 1 min. Curves were fitted using a second-order equation for a bimolecular reaction, 2(monomer) ⇔ dimer (Fersht, 1985):

$$\frac{1}{[\text{monomer}]_0 - [\text{dimer}]} - \frac{1}{[\text{monomer}]_0} = kt \qquad (1)$$

where $[\text{monomer}]_0$ is the concentration of monomeric species at time 0 and k is the second-order rate constant.

Cross-Linking Experiments. Barnase at a concentration of 56 μM was incubated in glycine buffer at 33 °C with and without 200 mM KCl. At different times of incubation, aliquots were taken and incubated in the presence of the cross-linker (20 mM) for a further 10 min. In order to remove the salts, the reaction was stopped by addition of 10% ice-cold trichloroacetic acid (Hames, 1981). The mixture was left on ice for 30 min, and the protein was collected after centrifugation. The pellet was washed with ethanol/ether (1:1), dried at room temperature, and redissolved in 20 mM 2-(*N*-morpholino)ethanesulfonic acid (Mes) buffer, pH 6.3. Samples were then analyzed by $NaDodSO_4$–PAGE according to Schägger and von Jagow (1987), and the protein bands were visualized with Coomassie Brilliant Blue (BDH). Samples were boiled for 5 min prior to electrophoresis.

RESULTS

Differential Scanning Calorimetry and Ionic Strength. At pH 4.0 and above, wild-type barnase and many mutants show essentialy fully reversible thermal unfolding at low ionic strength, with a van't Hoff to calorimetric enthalpy ratio

[1] Abbreviations: DSC, differential scanning calorimetry; ANS, 1-anilinonaphthalene-8-sulfonic acid; CD, circular dichroism; UV, ultraviolet; [θ], ellipticity; $NaDodSO_4$–PAGE, electrophoresis in polyacrylamide gels in the presence of sodium dodecyl sulfate; T_m, temperature of mid-completion of the transition; ΔH_{vh}, van't Hoff enthalpy; ΔH_{cal}, calorimetric enthalpy; EDAC, 1-ethyl-3-[3-(dimethylamino)propyl]-carbodiimide.

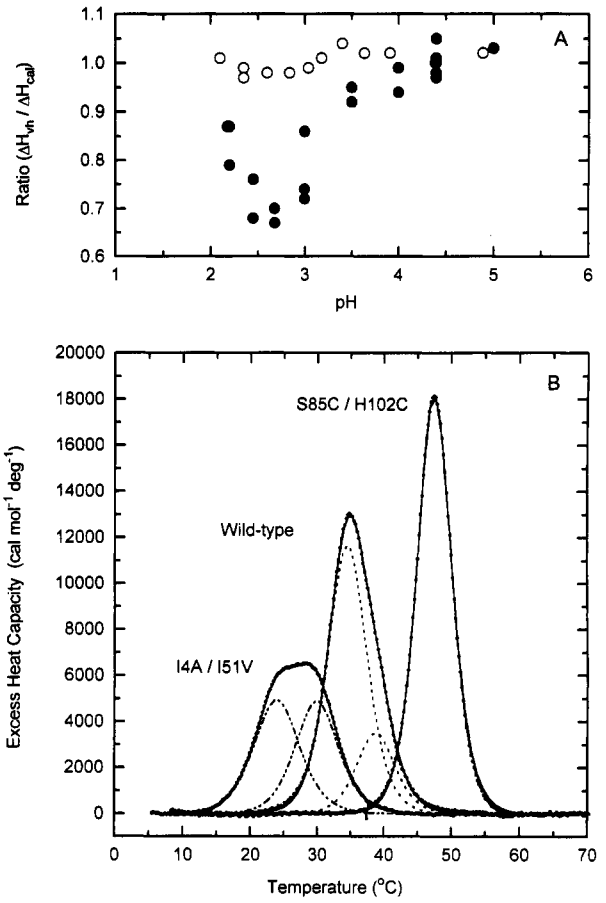

FIGURE 1: (A) Dependence of the van't Hoff to calorimetric enthalpies ratio of wild-type barnase on pH. DSC experiments were carried out at a protein concentration ranging from 40 to 50 μM in 20 mM buffer using acetate (pH > 4.0), formate (3.0 < pH < 4.0), or glycine (pH < 3.0) systems in the absence (closed circles) or in the presence (open circles) of 100 mM KCl. (B) DSC thermograms of different barnase mutants in glycine buffer, pH 2.7. The excess heat capacity plots were obtained as described in Materials and Methods and show the double mutant S85C/H102C (a-type), wild-type barnase (b-type), and the double mutant I4A/I51V (c-type). Results were obtained in 20 mM glycine buffer at a scan rate of 60 °C/h. Experimental points are represented as closed circles. Solid lines are the best fits of the data from deconvolution of the transitions, with the dashed (wild-type) and double dash/long dash (I4A/I51V) lines representing individual contributions to the fit where more than one transition was indicated.

($\Delta H_{vh}/\Delta H_{cal}$) of 1 (Matouschek et al., 1994). The T_m and molar enthalpies are independent of the protein concentration between 20 and 60 μM. These observations demonstrate that the thermal denaturation is a two-state equilibrium under these conditions. Below pH 4.0, the transition for wild-type barnase is still reversible but has a ratio $\Delta H_{vh}/\Delta H_{cal} < 1$ when fitting the curves to a single non-two-state calorimetric transition, reaching a minimum value of ~0.67 at pH 2.7 (Figure 1A). Total reversibility, together with native gel electrophoresis analysis of the heated samples, suggests that barnase does not undergo any chemical modification under the conditions of the experiments (data not shown). Addition of 100 mM KCl restores the $\Delta H_{vh}/\Delta H_{cal}$ ratio to 1 under these conditions.

Several barnase mutants were examined by DSC at pH 2.7. The results can be divided into three cases (*a*, *b*, and *c*), as summarized in Figure 1B. The mutant S85C/H102C (Clarke & Fersht, 1993) has an engineered disulfide bridge. In its oxidized form it yields a thermal transition with $\Delta H_{vh}/\Delta H_{cal}$ = 0.95 (Figure 1B). So far, this is the only mutant

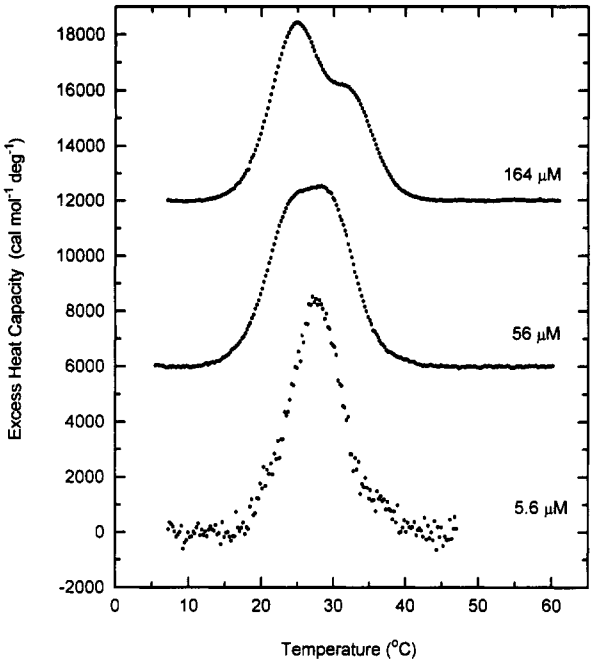

FIGURE 2: Effect of the protein concentration on the DSC thermogram of the I4A/I51V mutant. Excess heat capacity plots were obtained as described in Materials and Methods, and the data are offset in the *y*-axis for ease of presentation. Results were obtained in 20 mM glycine buffer at a scan rate of 60 °C/h.

whose DSC thermogram shape appears to be essentially independent of pH. Wild-type barnase shows a somewhat asymmetrical thermogram (Figure 2B). This is also the case for most barnase mutants analyzed at pH 2.7 (data not shown). Since fitting to a single two-state transition did not give satisfactory results, we tried deconvolution into mutiple contributions, but only two non-two-state transitions in which ΔH_{vh} and ΔH_{cal} were varied independently were found to fit the data satisfactorily (Figure 1B, Table 1). The first transition accounts for ~ 80% of the total heat absorbed. Finally, some mutants show a more complex, broader heat absorption curve (Figure 1B) that can also be fitted as the contribution of two independent non-two-state transitions, the second one accounting for ~ 50% of the heat absorbed (Table 1). However, this deconvolution may be made only in a qualitative manner, since equilibrium thermodynamic analysis cannot be used, despite the reversibility of these transitions (see below). Interestingly, the proteins exhibiting the latter behavior were the double mutants I4A/I51V and I4A/Y78F, as well as the quadruple mutant I4A/I25V/I51V/Y78F (data not shown), which have previously been shown to accumulate significant amounts of the major kinetic folding intermediate at equilibrium in the presence of urea (Sanz & Fersht, 1993). This fact suggests that the broadness of the DSC transition could be related to the ability of the mutation to stabilize the kinetic intermediate state. The fact that the latter three mutants share the mutation I4A raises the possibility that this mutation is responsible itself for the unusual calorimetric behavior. However, the double mutant I4A/I76V displays a *b*-type behavior (Table 1).

Heterogeneity in the samples could give rise to different populations undergoing different transitions during thermal unfolding. However, this possibility can be eliminated, since all the proteins were purified to >95% purity based on gel electrophoresis, and the same preparations showed a two-state transition when examined at pH 4.4 (data not shown).

Table 1: Thermal Characteristics of Barnase at pH 2.7

protein[a]	probe	heating rate (°C/h)	addition	T_m (°C)[b]	T_{m1} (°C) [%][c]	T_{m2} (°C) [%][c]	ΔH_{cal} (kcal/mol)[d]
S85C/H102C	DSC	60		47.4			125
wild-type	DSC	60			35.0 [74]	39.0 [26]	110
I4A/I76V	DSC	60			28.2 [76]	33.3 [24]	88
I76T	DSC	60			26.7 [83]	32.2 [17]	97
I4A/Y78F	DSC	60			25.4 [46]	29.8 [54]	81
I4A/I25V/I51V/Y78F	DSC	60			14.5 [52]	19.9 [48]	31
I4A/I51V	DSC	60			23.9 [53]	30.0 [47]	88
	DSC	30			22.0 [20]	27.1 [80]	70
	DSC	60	20% glycerol		25.7 [82]	31.3 [18]	96
	DSC	60	200 mM KCl	25.5			79
	DSC	20	200 mM KCl	25.4			82
	CD	50		28.9			
	CD	20		29.3			
	CD	50	20% glycerol	30.7			
	CD	50	200 mM KCl	25.7			

[a] Protein concentration was ~50 μM. [b] Temperature of the maximum of the heat capacity function. [c] Temperature of the maximum heat capacity from multiple deconvolution (1: first deconvolution; 2: second deconvolution). The area of the deconvolution as a percentage of the total area of the transition is shown in brackets. [d] Total heat absorbed in the calorimetric transition.

No macroscopic precipitation occurred during the DSC scans since these were fully reversible and the solutions heated to 105 °C remained optically clear. Both CD (see below) and NMR spectroscopy (not shown) of the proteins in the folded state at low pH show no significant structural deviation compared to the same state at pH 6.3. If the folded state were aggregating, it certainly does not seem to show a conformational change which might be great enough to explain a 5–6 °C difference in the thermal stability between the two deconvolutions (Table 1). Moreover, Makarov et al. (1992) have analyzed the structure of the folded state of barnase at pH 2.4 by analytical centrifugation and have concluded that barnase is not aggregating, but instead undergoes a decrease in the degree of compactness.

Interestingly, the precise geometry of the calorimetric cell seems to have an effect on the shape of the DSC transitions. No deviations from the two-state behavior have been found for barnase at low pH when capillary-type cells are used (Martinez et al., 1994), although distortions are seen when using lens-shaped cells (Makarov et al., 1992; this work). This effect is an intriguing observation for which we do not have an explanation. However, this phenomenon does not affect our analysis since the shapes of DSC transitions are only used in this study qualitatively and as an indicator of atypical behavior.

All the DSC transitions shown above were >95% reversible when rescanned after cooling. However, in order to analyze the curves according to equilibrium thermodynamic equations, thermal unfolding must be independent of the scan rate and the concentration of protein. Whereas *a*- and *b*-type traces are virtually independent of the scan rate, *c*-type transitions exhibit some dependence on these parameters. The lower the scan rate, the bigger is the apparent weight of the second deconvolution (Table 1). Moreover, *c*-type traces are also strongly dependent on the protein concentration; the most concentrated samples show clearly two separate heat absorption peaks (Figure 2) while at lower concentrations the thermograms resemble a two-state transition. Some of the samples corresponding to the *b*-type, like wild-type, do not show any appreciable change, whereas other mutants, like I76T, display a *c*-type pattern when the protein concentration is very high (data not shown). These data together suggest that the thermal unfolding of barnase, and in particular, the mutants described, at pH 2.7 involves slow, multimolecular equilibria that cannot be analyzed with the usual equilibrium equations. Deconvolution of the data into non-two-state transitions (Table 1) is therefore used purely as a phenomenological description and does not imply any true thermodynamic significance.

As illustrated in Figure 1A, the addition of 200 mM KCl changes the $\Delta H_{vh}/\Delta H_{cal}$ ratio for wild-type barnase to unity when heated at a rate of 60 °C/h. Salt has the same effect on all of the mutants, including the *c*-type ones. For example, the effect of KCl on the thermogram of the I4A/I51V mutant when heated at a scan rate of 60 °C/h is shown in Figure 3. The scan was ~ 95% reversible. The width of the transition decreases dramatically, regaining a $\Delta H_{vh}/\Delta H_{cal}$ ratio close to 1 (0.95) with a temperature of mid-completion (T_m) of 25.5 °C (Table 1). This is close to the T_m of the first of the two possible deconvolutions of the low ionic strength thermogram (Figure 1B, Table 1). Only minor changes in T_m were found for wild-type and S85C/H102C proteins in the presence of 200 mM KCl (data not shown). Interestingly, addition of 20% glycerol (a polar but nonionic agent) to the I4A/I51V mutant in the absence of KCl also produced a marked decrease in the asymmetry of the DSC transition (Figure 3A).

At a scan rate of 20 °C/h, dramatic and different changes were seen in the presence of 200 mM KCl for the I4A/I51V mutant (Figure 3B). The transition around 25 °C was conserved, but the heat capacity of the final state was lower than the post-transitional level when heated at 60 °C/h and very similar to that of the initial folded state. This result suggests that nonpolar groups of the protein are shielded from the solvent after the transition. Above 55 °C, there is a gradual increase in the heat capacity that finally coincides with that of the higher scan rate sample. No significant heat absorption peak was detected. Upon rescan the transition was only ~ 70% reversible, although the pattern of post-transition base lines was conserved (data not shown).

Fluorescence Studies. Changes in the tertiary structure of barnase upon increasing temperature were monitored by intrinsic tryptophan fluorescence (Figure 4). Loss of fluorescence at 315 nm follows a sigmoidal transition and was >95% reversible when the same sample was heated for a second time, thus eliminating the possibility of photolysis. The temperature of the midpoint of the transition varies depending on the concentration of protein, ranging from 24.5 °C at 2 μM to 27.0 °C at 56 μM for the I4A/I51V mutant (data not shown), suggesting association processes.

The fluorescent dye ANS is commonly used as a probe for accessible hydrophobic patches in proteins since its quantum yield increases when bound to such hydrophobic cores

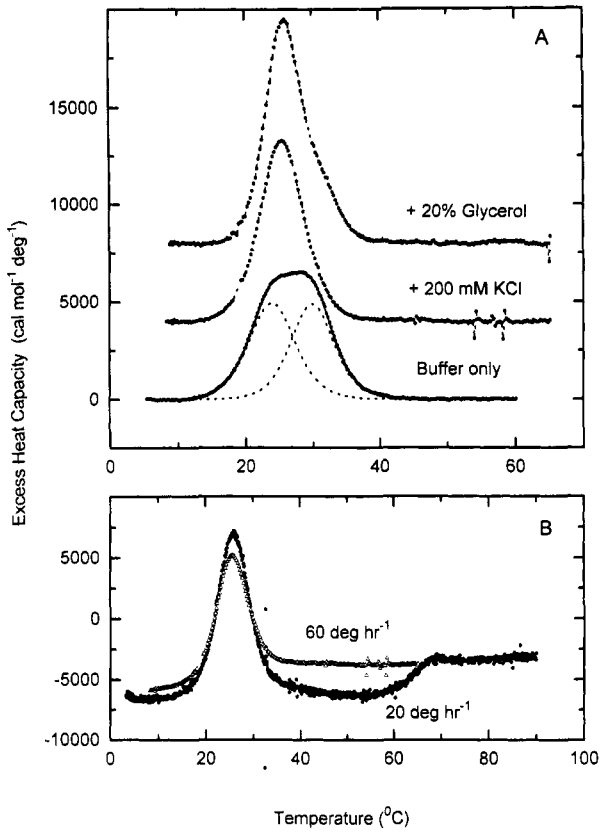

FIGURE 3: Effect of solvent conditions and scan rate on the DSC thermogram of the I4A/I51V mutant. Excess heat capacity plots were obtained as described in Materials and Methods and show (A) Data in glycine buffer only, in the presence of 20% glycerol, and in the presence of 200 mM KCl. The scan rate was 60 °C/h. (B) Effect of the scan rate in the presence of 200 mM KCl. The data are corrected by subtraction of buffer base lines and are concentration normalized but have not been processed to remove the denaturational heat capacity increment (see Materials and Methods). The protein concentration was 56 μM throughout.

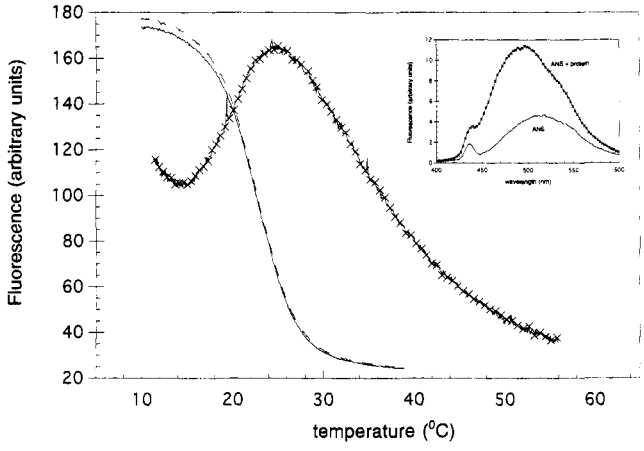

FIGURE 4: Thermal denaturation of the I4A/I51V mutant monitored by fluorescence spectroscopy. Barnase (2 μM) was heated in the presence of 20 μM ANS at ~ 60 °C/h. Tryptophan fluorescence at 315 nm was measured (solid line). A rescan of the same sample is shown in the dashed line. In a parallel sample, ANS fluorescence at 480 nm was measured (– × –). Inset: Binding of ANS to the folded state of the I4A/I51V mutant at 10 °C (excitation wavelength 380 nm).

(Semisotnov et al., 1991). Barnase does not bind ANS at pH 6.3 and 25 °C (Sanz & Fersht, 1993). However, we found some binding to the protein (2 μM) at pH 2.7, 5 °C, for wild-type and all mutants tested (Figure 4, inset). Use of a barnase concentration higher than 4 μM leads to the precipitation of the protein. Bound ANS has an increase in fluorescence quantum yield as well as a blue shift in the spectrum maximum. Since the far- and near-UV CD spectra of the folded protein recorded at both pHs are indistinguishable (see below), we think that protonation of some residues or ANS itself could make some hydrophobic parts of the protein accessible to the molecules of the dye without the need of a large conformational change.

The ANS fluorescence increases upon increasing temperature, reaching a maximum, and then decreases slowly (Figure 4). The maximum of ANS fluorescence occurs when about 85% of the tryptophan fluorescence is already lost. This result suggests the existence of accessible hydrophobic patches even though tertiary structure is absent. Binding does not affect the stability of the protein since the tryptophan fluorescence curves obtained in both the absence and the presence of the ligand are indistinguishable and equally reversible, and no significant differences are found when 200 mM KCl is present either (data not shown). Although the mutant I4A/I51V was the most extensively studied, many other mutants tested, including wild-type, show a similar behavior.

Thermal Denaturation Followed by Circular Dichroism. The stability of the secondary structure of barnase was monitored by following the ellipticity at 222 nm. Figure 5 shows the curves belonging to the I4A/I51V double mutant obtained using a protein concentration of 56 μM and a scan rate of 50 °C/h. Although the best signal in the far-UV CD spectrum of barnase is located around 230 nm, this band arises from the contribution of the tertiary environment of the side chain of Trp-94 (Vuilleumier et al., 1993), so that, despite the smaller signal, we chose instead the ellipticity at 222 nm ($[\theta]_{222}$) to monitor conformational changes in the secondary structure of the protein.

Thermal unfolding of barnase proceeds through a net increase in the intensity of $[\theta]_{222}$; *i.e.*, the signal becomes more negative compared with that of the folded state. This is not surprising since the CD spectrum of barnase has a very low intensity itself (Vuilleumier et al, 1993) and the spectra of thermally denatured proteins are different from those of urea- or guanidine hydrochloride-denatured polypeptides (Privalov et al., 1989). For the double I4A/I51V mutant at 56 μM, there is a low-intensity change in ellipticity with a T_m of 28.9 °C, followed by a highly sloping base line (Figure 5A, Table 1). Scans were completely reversible. Other *b*- and *c*-type proteins, including wild-type, showed a similar trend. In the presence of 20% glycerol, the transition itself accounts for a larger change in $[\theta]_{222}$ and an increase in T_m. The second base line is also more flat (Figure 5A, Table 1). However, marked differences are found in the presence of 200 mM KCl (Figure 5B, Table 1). After the completion of a transition with a lower T_m, there is a larger increase in the negative value of $[\theta]_{222}$ that levels off at about 60 °C and decreases after that temperature. Upon cooling, the original spectrum is not fully regained and a rescan of the same sample showed a decreased amplitude in the first transition although conserving the T_m (data not shown). At a protein concentration of 2 μM a decrease in T_m with respect to the sample in the absence of salt was also seen, but the base line peculiarities were not observed (data not shown). The traces of the *a*-type mutant S85C/H102C at 56 μM concentration exhibit a larger amplitude change on ellipticity than the I4A/I51V mutant (Figure 5C), as well as a post-transitional base line with a reduced slope. Addition of KCl somewhat increases the amplitude of the transition, but unlike I4A/I51V the changes in T_m are small.

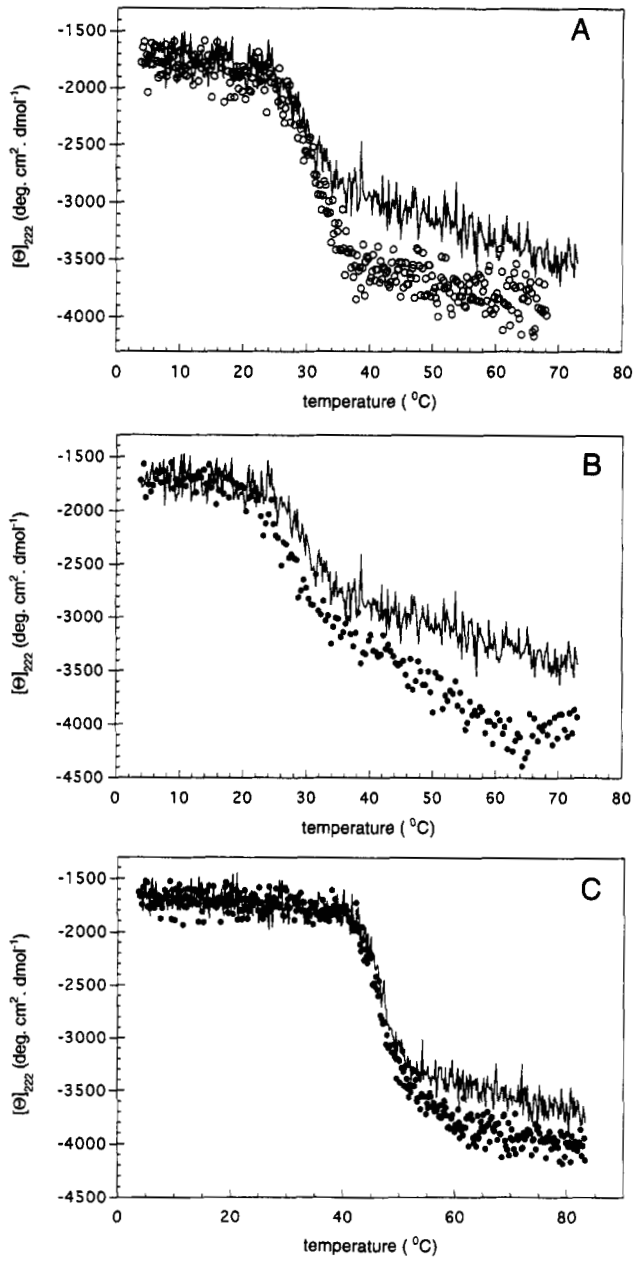

FIGURE 5: Thermal denaturation of barnase in glycine buffer monitored by CD. The barnase concentration was 56 μM, and the heating rate was 50 °C/h. (A) I4A/I51V mutant in the absence (solid line) and in the presence (open circles) of 20% glycerol. (B) I4A/I51V mutant in the absence (solid line) and in the presence (closed circles) of 200 mM KCl. (C) S85C/H102C mutant in the absence (solid line) and in the presence (closed circles) of 200 mM KCl.

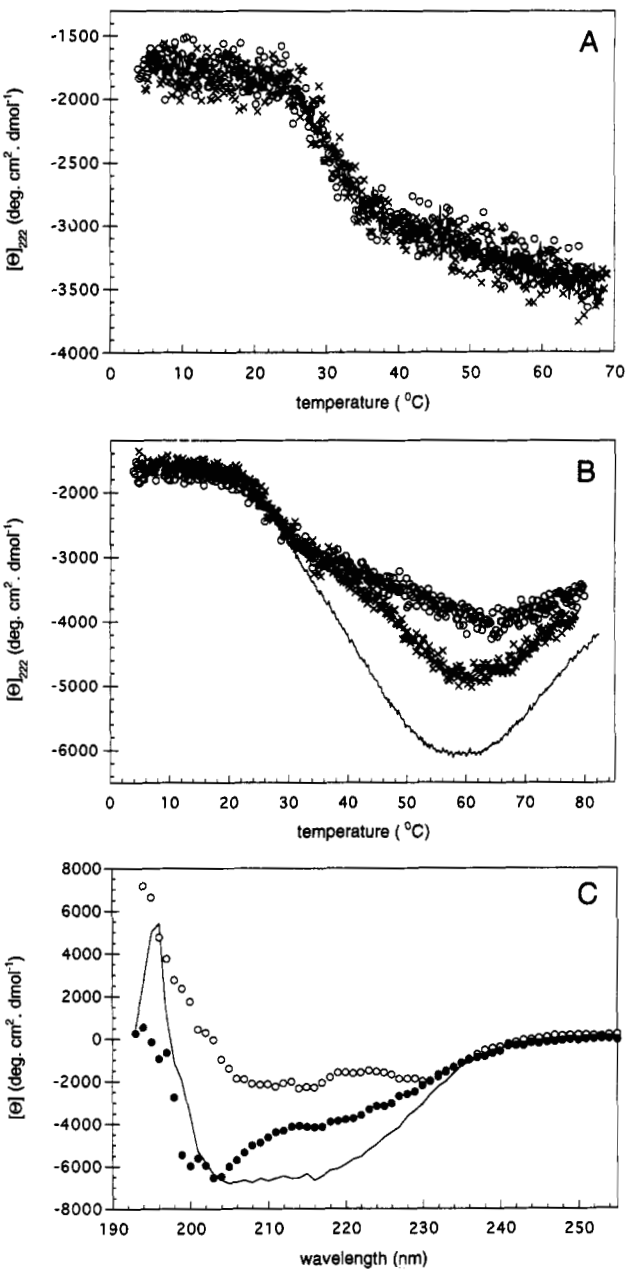

FIGURE 6: Effect of the heating rate on the denaturation of the I4A/I51V mutant monitored by CD. The barnase concentration was 56 μM. (A) Thermal denaturation in glycine buffer using a heating rate of 50 (open circles), 20 (crosses), and 10 (solid line) °C/h. (B) Thermal denaturation in glycine buffer plus 200 mM KCl. Conventions as in (A). (C) Thermal denaturation in glycine buffer plus 200 mM KCl. CD spectra taken at 5 °C (open circles), 50 °C (solid line), and 80 °C (filled circles) when the heating rate was 10 °C/h.

Since there is a significant kinetic control of the thermal denaturation of the mutant I4A/I51V followed by DSC in low and high ionic strength (Table 1, Figure 3B), we examined the effect of the heating rate on the CD curves at 50, 20, and 10 °C/h (Figure 6A,B). The protein concentration was fixed at 56 μM. Only minor changes in the pattern of denaturation were found at low ionic strength (Figure 6A, Table 1). In the presence of 200 mM KCl, however, a slower heating rate produces a higher sloping base line, to such an extent that it overlaps with the transition (Figure 6B). Upon cooling down to 5 °C the original CD spectrum is not fully regained (data not shown). Wavelength scans taken at several temperatures during the slow scans showed the appearance of a broad CD band that eventually disappears above 60 °C, after which the spectrum is more similar to that of a corresponding thermally unfolded protein (Figure 6C). No changes whatsoever were detected in the near-UV region above the transition zone (data not shown), and no macroscopic precipitation of the protein or change in the pH was found after the scans. The *c*-type mutant I4A/I78F exhibited a similar behavior, but no such effects were observed in wild-type barnase (data not shown).

Production of an Oligomeric A-State. From the results above, it is evident that the thermal denaturation of barnase at pH 2.7 is not a straightforward two-state process but involves multimolecular slow equilibria. Addition of KCl leads to large changes in the profile of the thermal transition when monitored by DSC or CD. Since it was likely that, even at the lowest scan rates, the equilibrium had not been reached satisfactorily, barnase was incubated for long times at different temperatures

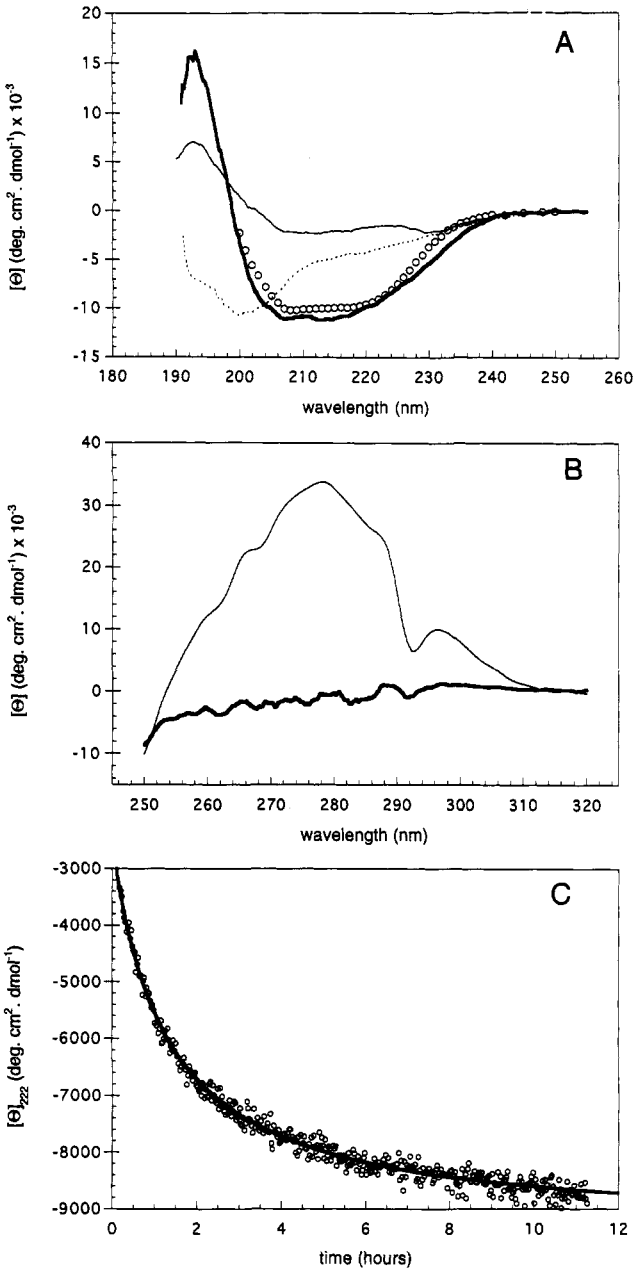

FIGURE 7: CD characteristics of the A-state of barnase (A) Far-UV CD spectra of the I4A/I51V mutant recorded at 5 °C, after 12 h incubation at 33 °C in glycine buffer, in the absence (solid line) and in the presence (thick line) of 200 mM KCl. The protein concentration was 56 μM. The spectrum of the thermally unfolded protein at 85 °C in glycine buffer only is shown (dashed line). The theoretical spectrum was generated (open circles) using the native secondary structure of barnase as determined by X-ray crystallography and the parameters of Bolotina et al. (1980) for CD contributions of pure secondary structures. (B) Near-UV CD spectra of the I4A/I51V mutant. Conditions and conventions as in (A). (C) Time course of the formation of the A-state. The I4A/I51V mutant at a concentration of 56 μM was incubated at 33 °C in glycine buffer in the presence of 200 mM KCl, and the ellipticity at 222 nm was measured every 20 s (response time = 2 s). Only one-fifth of the points are shown. Fitting to a second-order equation is shown by the thick line.

in the presence or absence of KCl, and the CD spectra following the incubation were recorded.

Figure 7A,B shows the resulting far- and near-UV CD spectra of the I4A/I51V mutant at 56 μM after 12 h incubation at pH 2.7, 33 °C, with and without 200 mM KCl. The samples were cooled down to 5 °C before CD measurements, well below the denaturation temperature of the folded state, in order to facilitate the comparison with the spectrum of the latter. However, only small differences were found after the incubation when the spectra were recorded between 5 and 50 °C. When salt is absent, the final spectra coincide with those of the folded state at pH 6.3, 25 °C (data not shown). However, dramatic changes can be seen in the sample with KCl. The far-UV CD spectrum displays a broad band with two minima centered at 207 and 215 nm, and a maximum at 194 nm (Figure 7A). The intensity of this band is considerably higher than that corresponding to the folded state but is different from the thermally unfolded one. The spectrum is indicative of a high content in secondary structure, and it bears resemblance to that obtained at intermediate temperatures when slowly heating up the protein (Figure 6C). However, there is no remaining signal in the near-UV region, indicating that the enviroment of the aromatic side chains of the protein is not different from that of the unfolded state (Figure 7B). Some presence of secondary structure and lack of fixed tertiary structure are characteristics of the so-called "molten globule" states (Ptitsyn, 1987). No state different from the folded form was found in the presence of KCl when the protein concentration was 2 μM, so the nature of the species generated in KCl must be multimolecular. This state of barnase, which we will hereafter term the A-state, is likely to be heterogeneous in terms of its oligomerization state, but we will refer to it generically as a single species. Its accumulation was successfully achieved between 30 and 45 °C after 12 h incubation, but outside this range the yield decreases notably, and, for example, after incubation at 5 °C virtually no change from the native spectrum was found (data not shown).

As shown in Figure 7A, we generated the predicted CD spectrum of barnase, whose secondary structure, according to X-ray crystallography, contains 22% α-helix, 22% β-structure, 14% turns, and 52% of other structures (Vuilleumier et al., 1993). We used the CD parameters of Bolotina et al. (1980) for pure secondary structures. The generated and the experimentally observed spectra of the A-state are nearly superimposable. This result indicates that the far-UV CD spectrum of the A-state can be explained in terms of the secondary structure of the native, fully folded protein, this is, the secondary structure of the A-state might be native-like.

Other mutants were tested for their ability to generate the A-state under the the above conditions. The *c*-type mutants (I4A/I51V, I4A/Y78F, and I4A/I25V/I51V/Y78F) all successfully produce the A-state (data not shown). I76T, a *b*-type mutant, does not yield the A-state when incubated at 56 μM, but formed a gel at 150 μM. On the other hand, wild-type does not show any deviation from the folded state upon incubation, even at 150 μM concentration. The A-state of I4A/I51V was also successfully induced by 50 mM potassium perchlorate, or at pH 0.7, which corresponds to a concentration of 200 mM HCl. However, 200 mM NaCl induced macroscopic precipitation of the protein (data not shown).

Glycerol, like KCl, induces a decrease in the asymmetry of the DSC thermogram of the I4A/I51V mutant (Figure 3A). However, a prolonged incubation of the mutant in the presence of 2.17 M glycerol does not lead to the A-state, nor does it inhibit its formation when 200 mM KCl was added (data not shown).

Characterization of Barnase A-State. In order to characterize the A-state of barnase, we studied the species obtained after incubating the I4A/I51V double mutant for 12 h at 33 °C in 20 mM glycine buffer in the presence of 200 mM KCl. We tried to overcome sample heterogeneity (*i.e.*, different degrees of oligomerization) by gel-filtration chromatography

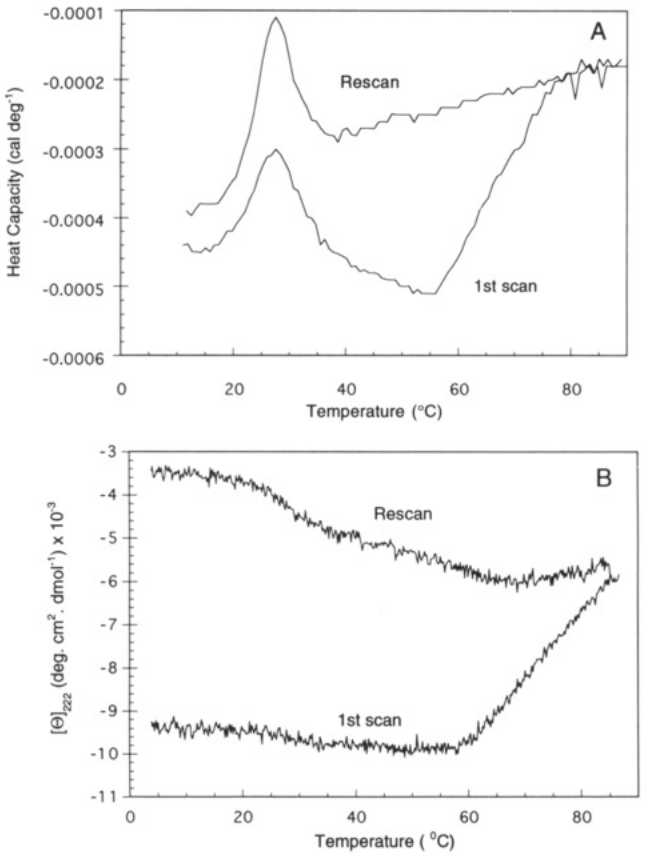

FIGURE 8: Thermal stability of the A-state. Thermal denaturation of the A-state in glycine buffer and 200 mM KCl. (A) DSC. The data have not been corrected by base line subtraction or normalized with respect to concentration. (B) Far-UV CD. The CD sample was an aliquot of the DSC sample. Heating rate was 60 °C/h (DSC) and 50 °C/h (CD). After the first scan, the samples were cooled to 5 °C and equilibrated at that temperature for 50 min. Then, a second scan was made, at the same heating rate. The A-state was obtained as described in the text from an initial monomer concentration of 56 μM.

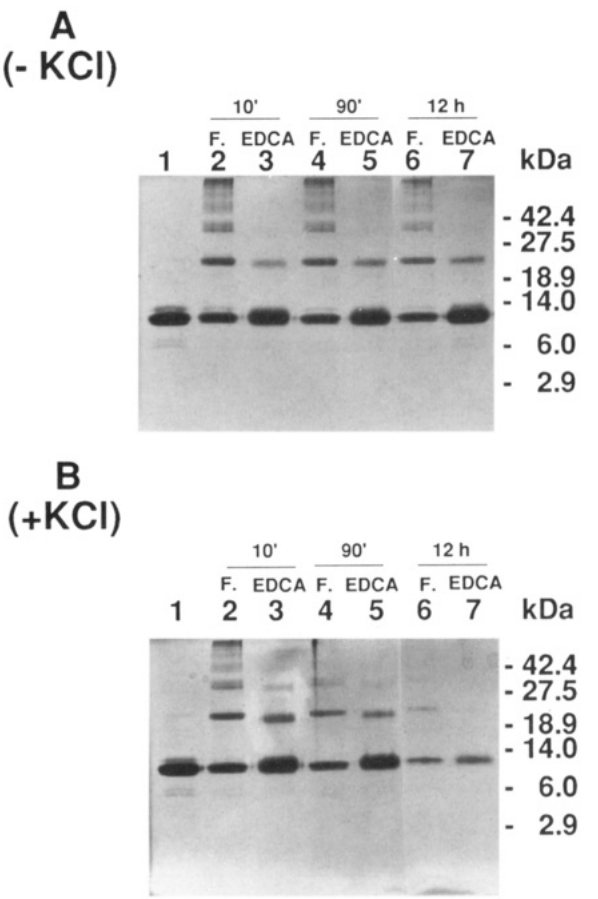

FIGURE 9: Covalent cross-linking of the I4A/I51V mutant. The protein was incubated at a concentration of 56 μM in glycine buffer in the absence (A) and in the presence (B) of 200 mM KCl. After the times shown in the figure, 20 mM formaldehyde (F) or EDAC was added. Samples were processed as described in Materials and Methods and were analyzed by NaDodSO$_4$–PAGE. Barnase in the absence of any cross-linking agent is shown as a control (lane 1).

of the incubated sample and further purification of the different peaks (see Materials and Methods). However, only peaks corresponding to the fully folded state could be seen (with a smaller intensity upon increasing time of incubation at low pH), whereas the partly folded forms remained bound to the chromatography supports and could not be released from the column unless 0.1 M KOH was used (data not shown).

A DSC thermogram of the A-state is shown in Figure 8A. A small intensity transition centered around 25 °C (probably indicative of remaining monomers that did not associate) is followed by a negatively sloping trace and then a positive one above ~60 °C. Upon rescanning the sample, the first transition increases in intensity, whereas the post-transition base line peculiarities are highly diminished. It is important to note the qualitative similarity of the first scan to the ones obtained by slowly heating up the folded state (Figure 3B). The thermal denaturation of an aliquot of the same A-state preparation was also monitored by far-UV CD in the presence of KCl (Figure 8B). There is a very small change around 25 °C, and when the temperature reaches 55 °C, the ellipticity is gradually lost in a noncooperative manner.

The results shown so far stress the fact that the concentration of the protein is an essential factor in obtaining the A-state of barnase. The A-state must be, then, oligomeric in nature. The kinetics of formation of the A-state may be useful in determining the order of the associated species. The time trace of formation of the A-state at 33 °C for the I4A/I51V mutant monitored by CD at 222 nm is shown in Figure 7C. Similar data were obtained at 25 °C for the I4A/I25V/I51V/Y78F mutant (data not shown). These two time traces can be satisfactorily fitted to a second-order equation (see Materials and Methods) with a rate constant in the range of 30–40 s^{-1} M^{-1}. This result suggests that the rate-limiting step is a bimolecular reaction. The difference in constants may be related to the different temperatures at which the experiments were carried out.

Cross-Linking Experiments. Three different cross-linking agents, namely formaldehyde, glutaraldehyde, and 1-ethyl-3-[3-(dimethylamino)propyl]carbodiimide (EDAC), were used to link covalently the associated species. In order to avoid the reaction of these compounds with the glycine present in the buffer, reactions were carried out at pH 2.7 adjusted with HCl. Formation of the A-state and its kinetics were previously found to be completely reproducible with HCl instead of glycine buffer (data not shown). The effect of formaldehyde and EDAC on the I4A/I51V mutant in the absence of KCl at 33 °C is shown in Figure 9A. Covalent cross-linking was achieved and produced, among others, species with an apparent molecular mass of ~ 25 kDa, that could correspond to a dimer of barnase. Formaldehyde appeared to be a stronger cross-linker than EDAC, since forms of higher M_r could be found in the former case. Similar results were found upon incubation at different times (10 min, 90 min, and 12 h), demonstrating that the equilibrium was achieved relatively fast and did not change even after longer periods

of incubation. Glutaraldehyde produces similar results to those of formaldehyde. The presence of the cross-linking agents during the incubation was found to inhibit the association reaction, probably by modifying some side chains needed for the reaction to occur (data not shown). When 200 mM KCl was present in the reaction (Figure 9B), the amount of dimers linked by formaldehyde is not higher compared with the levels observed in the absence of salt, but a significant decrease of monomeric species is evident at longer incubation times, suggesting the formation of higher order forms that are not able to enter the polyacrylamide gel. Indeed, an intense Coomassie Blue-stained band was found in the wells of the gel in such cases. Alternatively, the modified side chains might be unable to bind $NaDodSO_4$ properly. EDAC has a more controlled reaction, and when incubated in the presence of KCl at short times (10 min), it produces, in addition to the 25 kDa band, a weak band of $\sim$ 42 kDa. This band could correspond to trimers of barnase ($\sim$ 37 kDa), although the possibility of tetramers ($\sim$ 49 kDa) with aberrant mobility due to the chemical modification of the side chains and/or more compactness induced by intramolecular cross-linking cannot be ruled out.

DISCUSSION

The structures of denatured proteins at low pH (A-states) have received considerable attention because of the attractive possibility that they might be stabilized kinetic folding intermediates that otherwise do not accumulate at equilibrium, although a definitive proof is elusive. Stopped-flow CD data of the refolding of staphylococcal nuclease A (Sugawara et al., 1991), α-lactalbumin (Kuwajima et al., 1985), and apomyoglobin (Jennings & Wright, 1993) suggest that the far-UV CD spectrum and the energetics of chemical denaturation of their refolding intermediates are similar to those of the corresponding A-states in equilibrium. However, some acidic states are unlikely to represent folding intermediates, but rather alternative folded structures. The A-states of barstar (Khurana & Udgaonkar, 1994) and the immunoglobulin MAK33 (Buchner et al., 1991) are much more stable than that expected for an intermediate (in some cases, even more stable than the folded state). Exotoxin A at acidic pH is even capable of adopting a functional conformation differing from that of the native protein (Jiang & London, 1990). Barnase is a suitable system in which to examine the behavior of proteins at low pH. A large number of mutants is available, and its pathway of folding is one of the best characterized (Matouschek et al., 1992a,b; Serrano et al., 1992; Fersht, 1993). The results presented here suggest that barnase thermally denatures at low pH through a complex pathway of slow, multimolecular and branched equilibria which are difficult to analyze quantitatively, not only because of the complexity, but also because equilibrium thermodynamics cannot be applied. However, some of the characteristics of these pathways can be deduced under certain conditions. We will try to explain the results according to the simplest model which is consistent with the observed behavior as depicted in Scheme 1.

Results at Low Ionic Strength. The behavior of barnase upon thermal denaturation above pH 4.0 and low ionic strength (20 mM) follows a two-state mechanism, according to the ratio of the van't Hoff and calorimetric enthalpies being close to 1 (Figure 1A). However, below pH 4.0, the heat absorbed is higher than that corresponding to a two-state process. The DSC thermograms become asymmetric and their shape is dependent on the mutant tested (Figure 1B), as well as on the concentration of protein and the scan rate (Table 1, Figure 2). All these data together suggest that the thermal denaturation of barnase at low pH involves slow, multiple equilibria concomitantly with self-association events. This fact prevents the use of equilibrium thermodynamics for the analysis of the transitions, so that all analysis must be made in a qualitative way.

Scheme 1

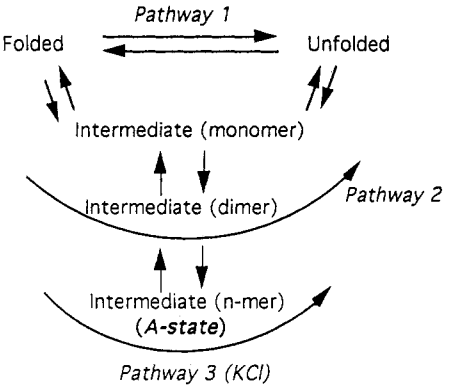

Mutants have been grouped as *a*-, *b*-, or *c*-type, according to the appearance of the DSC transitions obtained at pH 2.7 (Figure 1B) at concentrations around 56 μM. The double mutant S85C/H102C (*a*-type) is the only mutant found so far that undergoes essentially a two-state transition ($\Delta H_{vh}/\Delta H_{cal} \sim 1$) irrespective of the pH. The most common case is the *b*-type trace, that exhibits a slightly asymmetric transition. The best fitting is achieved upon deconvolution to two non-two-state transitions, either consecutive or not, the second one being of lower intensity. The *c*-type proteins display a much larger second transition. The only *c*-type proteins are I4A/I51V and I4A/Y78F, and the quadruple mutant I4A/I25V/I51V/Y78F, which were designed to accumulate the major kinetic folding intermediate of barnase under certain concentrations of urea (Sanz & Fersht, 1993). According to Scheme 1, barnase can denature via two possible pathways branching out from the folded state. If little intermediate accumulates, most of the molecules denature via pathway 1 and only a small part take the side route, giving rise to a small asymmetry in the calorimetric peak. If more intermediate is present, the proportions of folded molecules undergoing different transitions produce a broader thermal transition, with more molecules taking pathway 2. Note that this pathway is itself complex and we do not try to assign it to any of the two calorimetric deconvolutions.

There is a marked effect of the concentration of the protein on the *c*-type DSC traces (Figure 2). A low concentration leads to a more two-state transition. This may be explained on the basis that as the concentration of the protein increases and sufficient intermediate accumulates, the self-association of the latter is promoted and gives rise to an enhanced broadness of the calorimetric transition. Instability alone is not sufficient to explain the broadness of the thermograms, since the mutant I76T is similarly unstable and does not show such great asymmetry in DSC data at the same concentrations (Table 1). In the *b*-type group, wild-type traces are independent of concentration up to 150 μM, but the mutant I76T exhibits some distortion at a concentration of 220 μM (data not shown).

The intrinsic fluorescence and the far-UV CD signal of the protein are lost upon thermal denaturation in a sigmoidal fashion (Figures 4 and 5). The temperature of mid-completion depends on the concentration of the protein and cannot be assigned to either of the two deconvolutions of the DSC traces,

but lies between the two (Table 1). These results suggest that the deconvolution procedure is probably an oversimplification of a more complex system. In contrast to pH 6.3, ANS is able to somewhat bind to folded barnase at pH 2.7. Protonation of some residues and/or ANS itself may make the hydrophobic core of the protein become accessible to the probe, and it is also likely that the folded state of barnase is less compact at low pH (Makarov et al., 1992). Upon increasing temperature, the quantum yield of ANS increases to a maximum and subsequently decreases. The maximum of ANS fluorescence occurs at a temperature higher than the T_m measured by tryptophan fluorescence, suggesting that such hydrophobic patches become increasingly accessible after the loss of fixed tertiary structure (Figure 4).

The thermal denaturation of barnase followed by far-UV CD shows a sigmoidal transition followed by a sloping base line. Differences in base lines and in the amplitude of the change in ellipticity are correlated to changes in the broadness of the DSC thermograms. For example, the mutant S85C/H102C displays a bigger amplitude change and a more reduced base line than I4A/I51V (Figure 5A,C). Also, an increase in amplitude and a decrease in the sloping base line for I4A/I51V are achieved in the presence of glycerol (Figure 5A), an agent that also reduces the width of the DSC transition (Figure 3A). This implies that the structure of the thermally denatured state is different depending on the mutant and the properties of the solution. A small amplitude of change and a highly sloping CD base line may be representative of the presence of partly structured states that do not denature cooperatively, as reflected in complex calorimetric behavior.

Existence of associating states in the thermal denaturation transition region can be characterized by covalent cross-linking and subsequent analysis in $NaDodSO_4$–PAGE gels. In addition to other species, formaldehyde cross-linking mainly produces a prominent band with a calculated molecular mass of 25 kDa (Figure 9A), that could be assigned to a dimer of barnase molecules. Formaldehyde has been described to mainly react with deprotonated amino groups, although it can also react with the side chains of cysteine, tyrosine, histidine, tryptophan, and arginine (Tae, 1983), which would explain the activity of the agent at a pH where all lysine side-chain amino groups should be protonated. EDAC behaves as a weaker cross-linker of carboxyl groups that allows a more controlled reaction. Again, the same 25 kDa band could be seen, but without the larger molecular weight species (Figure 9A). This result demonstrates that dimers of barnase are formed specifically on thermal denaturation at pH 2.7.

Results at High Ionic Strength. The most obvious effect of the addition of 200 mM KCl to wild-type barnase is to produce an apparent two-state DSC transition (Figure 1A). A similar effect is observed for the double mutant I4A/I51V (Figure 3A). These results would suggest that KCl could be reverting any association process and destabilizing any intermediate states, such that denaturation proceeds mainly through pathway 1. However, this assumption is not necessarily correct. Although >95% reversibility is achieved for I4A/I51V when the DSC scan rate is 60 °C/h, only ~70% of the DSC cooperative transition was observed upon rescanning when the rate was 20 °C/h. At this heating rate, the post-transitional heat capacity turns out to be lower than in the case of faster heating, and very similar to that of the folded state, suggesting that nonpolar groups are still buried and shielded from water (Figure 3B) in a kind of denatured (but not fully unfolded) state which is formed in a slow time scale after the major cooperative transition (Privalov & Makhatadze, 1990). For far-UV CD-monitored thermal denaturation, KCl somewhat increases the amplitude of change for wild-type and the S85C/H102C mutant, but any change in T_m is very small (Figure 5C, Table 1). In contrast, the effects of salt on the *c*-type proteins are much greater (Figure 5B). As well as a larger amplitude, a decrease in T_m is seen, in agreement with the DSC thermogram (Figure 3A, Table 1).

During scanning at 20 °C/h in the presence of KCl, the I4A/I51V mutant shows a lowered heat capacity after the main DSC transition that is maintained up to 60 °C (Figure 3B). There is a remarkable similarity between this and the thermal denaturation monitored by CD (Figure 6B). In this case, conformational changes can be seen that give rise to species displaying an intense CD band (Figure 6C). According to Scheme 1, a major accumulation of intermediate would be produced during the major cooperative transition. Self-association of the intermediate would occur in a slow time scale, but the product (the A-state) would be extremely stable and the equilibrium is displaced to this state until the temperature reaches 60 °C. In contrast, when the sample is scanned at 60 °C/h, unfolding of the intermediate is faster than its self-association and therefore most of the molecules denature through pathway 1. During slower heating rates a dissociation of the accumulated A-state occurs above 60 °C. The CD spectrum at high temperature resembles that corresponding to a heat-unfolded protein (Figure 6C), and the heat capacity increases monotonically reaching the expected values for a completely unfolded barnase (Figure 3B). In this context, it is noted that the dissociation event proceeds without any significant heat absorption peak resembling a second-order calorimetric transition, *i.e.*, one that occurs with changes in the second derivative of the thermodynamic potential, that is, the heat capacity (Griko & Privalov, 1994). However, the lack of cooperativity may also be due to the heterogeneity of the initial A-state as well as a high number of possible different intermediate species that originate in the deassociation process (Griko et al., 1994).

Characterization of the A-State of Barnase. The oligomeric A-state of barnase in the presence of KCl can be observed with the *c*-type mutants I4A/I51V, I4A/Y78F, and I4A/I25V/I51V/Y78F. The time course of the self-association reaction at a fixed temperature just above their calorimetric transition can be fitted to a second-order reaction equation (Figure 7C), so the rate-limiting step may be bimolecular. However, the final state after incubation does not seem to be a dimer, as cross-linking experiments suggest (Figure 9B). Very little protein is seen in the gels after 12 h incubation using any of the cross-linking agents, unlike the situation at low ionic strength. High molecular weight, covalently cross-linked complexes are not able to enter the polyacrylamide gel and remain in the gel wells, although it may also be possible that such complexes are not very big, but are chemically modified in such a way that they are thus not properly unfolded in the $NaDodSO_4$–PAGE conditions. A possible explanation for the order of the reaction is that, once the dimer is formed, any further association is fast in comparison to the formation of bimolecular species which then becomes the rate-limiting step.

The far-UV CD spectrum of the A-state displays a broad band with minima centered at 215 and 207 nm (Figure 7A). The ellipticity at 222 nm is about 4 times higher than in the absence of salt. This spectrum is not similar to the spectra described for acid- or thermally-unfolded proteins, which generally display a minimum around 200 nm (Privalov et al.,

1989), or that observed for barnase in the absence of salt (Figure 7A). Such an intense change in the far-UV CD signal when compared to the spectrum of the folded state might indicate that the secondary structure of the A-state is not native-like. However, the CD spectrum of native barnase is itself atypical, with extensive canceling out of bands with positive and negative ellipticities, some of them very likely arising from tertiary structure contributions (Vuilleumier et al., 1993). The spectra are thus very difficult to analyze with the usual structural deconvolution algorithms. Removal of such unusual contributions in the conditions used for the stabilization of the A-state could unveil the expected spectrum of barnase. In fact, a simulated CD spectrum generated on the basis of the secondary structure of the protein is nearly coincident with the experimental spectrum of the A-state (Figure 7A), suggesting that the A-state is built from monomers with native-like secondary structure that achieve stabilization by intermolecular association. On the other hand, the lack of near-UV CD shows that there is not a fixed environment for the aromatic side chains in the A-state (Figure 7B). Current probes for tertiary structure only indicate the environment of aromatic residues (near-UV CD, fluorescence) so possible interactions involving other kinds of residues may be silent to these techniques. Such contacts may be responsible for the association of the barnase A-state. The acidic states of CheY (Filimonov et al., 1993) and creatinase (Schumann & Jaenicke, 1993) are oligomeric in nature, and although no near-UV CD signal differences from those of the unfolded state can be detected, tertiary (or at least supersecondary) contacts must be present.

In summary, it can be concluded from this study that the A-state of barnase shows some of the characteristics of the so-called "molten globule" states, *i.e.*, high content of secondary structure, no fixed tertiary structure, and a lack of cooperativity upon thermal denaturation. Also, ANS increases its fluorescence when binding to a low concentration of protein (2 μM) which is insufficient to promote the oligomeric A-state. We believe that the monomers and dimers of the intermediate state of barnase that are formed in the transition region are the species responsible for the increasing binding of ANS, thus revealing a more accessible hydrophobic core to the solvent, and may also possess themselves the features of molten globules.

REFERENCES

Barrick, D., & Baldwin, R. L. (1993) *Protein Sci. 2,* 869–876.

Bolotina, T. A., Chekhov, V. O., Lugauskas, V. Y., & Ptitsyn, O. B. (1980) *Mol. Biol. (Moscow) 14,* 902–908.

Buchner, J., Renner, M., Lilie, H., Hinz, H.-J., Jaenicke, R., Kiefhaber, T., & Rudolph, R. (1991) *Biochemistry 30,* 6922–6929.

Bychkova, V. E., & Ptitsyn, O. B. (1993) *Chemtracts Biochem. Mol. Biol. 4,* 133–163.

Bychkova, V. E., Berni, R., Rossi, G. L., Kutyshenko, V. P., & Ptitsyn, O. B. (1992) *Biochemistry 31,* 7566–7571.

Clarke, J., & Fersht, A. R. (1993) *Biochemistry 32,* 4322–4329.

Creighton, T. E. (1986) *Methods Enzymol. 131,* 83–106.

Creighton, T. E. (1990) *Biochem. J. 270,* 1–16.

Dill, A. K. (1985) *Biochemistry 24,* 1501–1509.

Fersht, A. R. (1985) *Enzyme Structure and Mechanism,* 2nd ed., W. H. Freeman & Co., New York, NY.

Fersht, A. R. (1993) *FEBS Lett. 325,* 5–16.

Filimonov, V. V., Prieto, J., Martinez, J. C., Bruix, M., Mateo, P. L., & Serrano, L. (1993) *Biochemistry 32,* 12906–12921.

Goto, Y., Takahashi, N., & Fink, A. L. (1990) *Biochemistry 29,* 3480–3488.

Griko, Y. V., & Privalov, P. L. (1994) *J. Mol. Biol. 235,* 1318–1325.

Griko, Y. V., Freire, E., & Privalov, P. L. (1994) *Biochemistry 33,* 1889–1899.

Hames, B. D. (1981) in *Gel Electrophoresis of Proteins: A Practical Approach* (Hames, B. D., & Rickwood, D., Eds.) IRL Press Ltd., London.

Haynie, D. T., & Freire, E. (1993) *Proteins: Struct., Funct., Genet. 16,* 115–140.

Hughson, F. M., Barrick, D., & Baldwin, R. L. (1991) *Biochemistry 30,* 4113–4118.

Jennings, P. A., & Wright, P. E. (1993) *Science 262,* 892–895.

Jiang, J. X., & London, E. (1990) *J. Biol. Chem. 265,* 8636–8641.

Khurana, R., & Udgaonkar, J. B. (1994) *Biochemistry 33,* 106–115.

Kim, P. S., & Baldwin, R. L. (1990) *Annu. Rev. Biochem. 59,* 631–660.

Kuroda, Y., Kidokoro, S., & Wada, A. (1992) *J. Mol. Biol. 223,* 1139–1153.

Kuwajima, K. (1989) *Proteins: Struct., Funct., Genet. 6,* 87–103.

Kuwajima, K., Hiraoka, Y., Ikeguchi, M., & Sugai, S. (1985) *Biochemistry 24,* 874–881.

Makarov, A., Protasevich, I., Kuznetsova, N., Fedorov, B., Korolev, S., Struminskaya, N., Leschinskaya, I., Yakoviev, G., & Esipova, N. (1992) in "Proceedings" from *Stability and Stabilization of Enzymes* (van den Tweel, W. J. J., Harder, A., & Buitelaar ed, R. M., Eds.) pp 377–381, Maastricht, The Netherlands.

Martinez, C., El Harrous, M., Filimonov, V. V., Mateo, P. L., & Fersht, A. R. (1994) *Biochemistry 33,* 3919–3926.

Matouschek, A., Kellis, J., Jr., Serrano, L., Bycroft, M., & Fersht, A. R. (1990) *Nature 346,* 440–445.

Matouschek, A., Serrano, L., & Fersht, A. R. (1992a) *J. Mol. Biol. 224,* 819–835.

Matouschek, A., Serrano, L., Meiering, E. M., Bycroft, M., & Fersht, A. R. (1992b) *J. Mol. Biol. 224,* 837–845.

Matouschek, A., Matthews, J. M., Johnson, C. M., & Fersht, A. R. (1994) *Protein Eng. 7,* 1089–1095.

Oas, T. G., & Kim, P. S. (1988) *Nature 336,* 42048.

Privalov, P. L., & Makhatadze, G. I. (1990) *J. Mol. Biol. 213,* 385–391.

Privalov, P. L., Tiktopulo, E. I., Venyaminov, S. Y., Griko, Y. V., Makhatadze, G. I., & Khechinashvili, N. N. (1989) *J. Mol. Biol. 205,* 737–750.

Ptitsyn, O. B. (1987) *J. Protein Chem. 6,* 273–293.

Sanz, J. M., & Fersht, A. R. (1993) *Biochemistry 32,* 13584–13592.

Schägger, H., & von Jagow, G. (1987) *Anal. Biochem. 166,* 368–379.

Schumann, J., & Jaenicke, R. (1993) *Eur. J. Biochem. 213,* 1225–1233.

Semisotnov, G. V., Rodionova, N. A., Razgulyaev, O. I., Uversky, V. N., Gripas, A. F., & Gilmanshin R. I. (1991) *Biopolymers 31,* 119–128.

Serrano, L., Horovitz, A., Avron, B., Bycroft, M., & Fersht, A. R. (1990) *Biochemistry 29,* 9343–9352.

Serrano, L., Matouschek, A., & Fersht, A. R. (1992) *J. Mol. Biol. 224,* 805–818.

Sugawara, T., Kuwajima, K., & Sugai, S. (1991) *Biochemistry 30,* 2698–2706.

Tae, H. J. (1983) *Methods Enzymol. 91,* 580–609.

Vuilleumier, S., Sancho, J., Loewenthal, R., & Fersht, A. R. (1993) *Biochemistry 32,* 10303–10313.

Yutani, K., Ogasahara, K., & Kuwajima, K. (1992) *J. Mol. Biol. 228,* 347–350.